PROJECTIONS OF FUTURE METEOROLOGICAL DROUGHT IN JAVA–NUSA TENGGARA REGION BASED ON CMIP6 SCENARIO

Afifah Huda SAFURA [1], ***Andung Bayu SEKARANOM*** [1*]

DOI: 10.21163/GT_2024.191.04

ABSTRACT:
Between 2018 and 2022, the primary regions for rice production in Indonesia were Java, Bali, and Nusa Tenggara, collectively contributing to approximately 61% of the annual rice production. Unfortunately, these islands are also most vulnerable to crop failure due to drought-induced water shortages. Therefore, this study predicted the occurrence, duration, and severity of meteorological drought in Java, Bali, and Nusa Tenggara using rainfall data from six climate models within the CMIP6 framework under the SSP245 and SSP585 scenarios. The observed data of 20 BMKG rainfall stations in the study area was acquired to adjust the output of the CMIP6 models using the Linear Scaling (LS) method. The Standardized Precipitation Index (SPI) at a 3-month scale (SPI-3) was used to analyze meteorological drought characteristics, such as frequency, duration, and intensity. The results showed that drought frequency increased and persisted for longer durations, particularly in the Nusa Tenggara region. However, compared to the observation period, drought intensity was predicted to decline in both scenarios compared to the observed period. The SSP585 scenario also indicated a higher level of drought compared to SSP245.

Key-words: *Meteorological drought, Drought characteristics, Climate change, CMIP6, SPI*

1. INTRODUCTION

Drought events are predicted to occur more frequently due to climate change, which acts as a triggering factor for increasing temperature variations and extreme rainfall. According to the Intergovernmental Panel on Climate Change (IPCC) Sixth Assessment Report (AR6), global surface temperature increased by 1.09°C from 2011 to 2020 compared to the period from 1850 to 1900 (IPCC, 2021), with the hottest years occurring between 2015 and 2019 (WMO, 2020). A 1°C increase in global temperature reduces rainfall by approximately 2% (Held & Soden, 2006; Liu et al., 2018) and has the potential to disrupt the water cycle (Huang et al., 2016). These changes in the hydrological cycle led to spatial-temporal variations in water availability, thereby triggering drought disasters. Consequently, several disaster events, including droughts, have been witnessed in recent decades (Cook et al., 2020; Kang et al., 2021).

EM-DAT, (2021), reported that drought accounted for 59% of the total economic losses caused by climate-related disasters. Furthermore, it had inflicted a devastating human toll, claiming 11.73 million lives between 1900 and 2021 (Li et al., 2021). Ha et al., (2022), stated that the agricultural sector is the most affected by climate-related disasters, as shown in the case of Indonesia, where approximately 389.19 thousand hectares of agricultural land experienced crop failure in 2019 (Indonesian Bureau of Statistics, 2020). The dry season in 2019 led to drought and crop failures, specifically in Java, Bali, and Nusa Tenggara. The occurrence of droughts in these regions is influenced by the El-Ninõ phenomenon in the Asia Pacific region (Kuswanto & Rahadiyuza, 2018). Given the severity of these issues, it is essential to identify future drought projections in Java, Bali, and Nusa Tenggara. Understanding the anticipated duration, severity, and intensity of future droughts is essential for formulating effective disaster risk management strategies at both local and national levels, alongside the implementation of adaptation measures.

[1]*Department of Environmental Geography, Faculty of Geography, Gadjah Mada University, 55281Yogyakarta - Indonesia; afifahhuda.safura@mail.ugm.ac.id; corresponding author* andung.geo@ugm.ac.id*

Several methods have been devised to predict meteorological drought characteristics, with the Standardized Precipitation Index (SPI) being a prominent choice in related studies (Zhai et al., 2020). Initially proposed by McKee et al. (1993), SPI was designed as a meteorological drought index but has since proven versatile in identifying agricultural and hydrological droughts (Parkhurst et al., 2019). Adhyani et al., (2017), stated that this method is also used to monitor and provide early warnings for drought. Predicting future droughts relies on climate projections generated concerning climate change scenarios. A significant player in climate modelling is the Coupled Model Intercomparison Project (CMIP), a subset of Global Circulation Models (GCMs). CMIP6, which is the most recent iteration, offers advanced ensemble simulations using the latest climate models (Eyring et al., 2016). It is believed to be highly accurate in reproducing global average precipitation patterns compared to CMIP3 and CMIP5 (Bock et al., 2020; Xin et al., 2020; Zhu et al., 2020). Based on this, recent studies have updated their assessments of climate change-related drought impacts using CMIP6 outputs. For example, Cook et al. (2020) reported increased evapotranspiration and the occurrence of extreme drought events in several regions by the end of the 21st century. Ukkola et al. (2020) found significant changes in the duration and frequency of seasonal meteorological droughts using CMIP6 projections. Similarly, Zhai et al. (2020) reported a significant increase in droughts within the Northwestern South Asia sub-region, characterized by prolonged durations and higher intensities from 2020 to 2099, using an ensemble average of five CMIP6 models under three distinct scenarios (SSP1–2.6, SSP2–4.5, and SSP5–8.5).

Java, Bali, and Nusa Tenggara Islands are significant producers of rice, accounting for about 61% of the country's total annual rice production from 2018 to 2022 (Indonesian Bureau of Statistics, 2023). However, these islands also face frequent drought disasters. Bali experienced frequent droughts between 2003 and 2012, affecting about 1,500 hectares of agricultural land (Muharsyah & Ratri, 2015). In 2017, droughts in Java and Nusa Tenggara affected numerous regions, including more than 2,500 villages in 100 regencies, and impacting more than 3.5 million people (Parkhurst et al., 2019). These droughts not only required clean water assistance but also posed a threat to crop failure in the agricultural sector. In 2019, approximately 400,000 hectares of agricultural land in Indonesia suffered crop failure, with the highest impact occurred in Java, Bali, and Nusa Tenggara Islands (Indonesian Bureau of Statistics, 2020). These findings highlight the challenges faced by these regions in balancing agricultural productivity and mitigating the effects of drought.

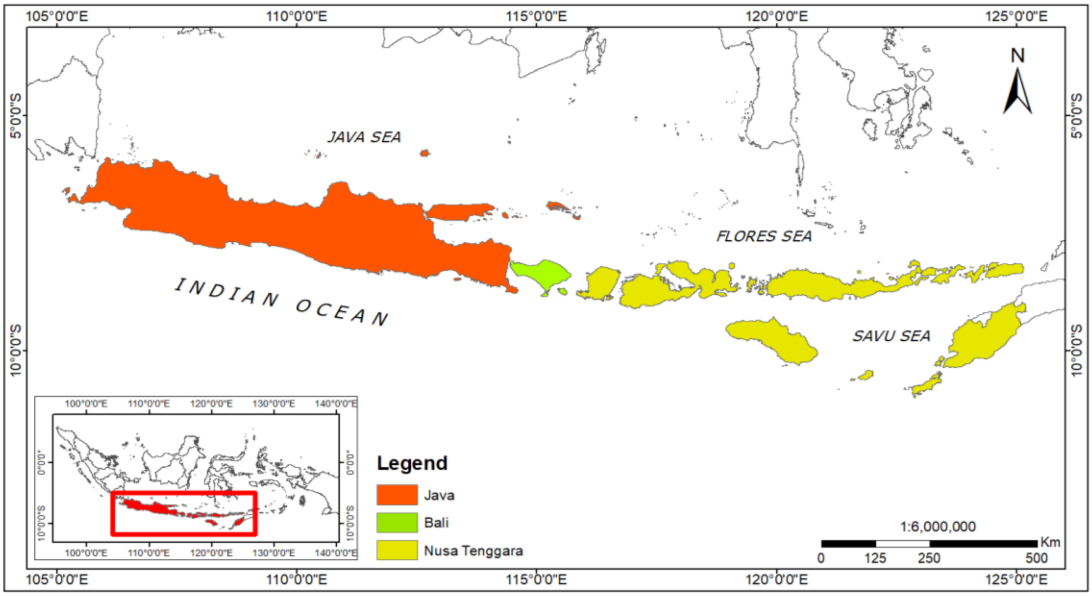

Fig. 1. The Map of Java, Bali, and Nusa Tenggara Islands as Study Area
(*Coastline data from GSHHG, 2017*).

In Indonesia, specifically in drought-prone regions like Java, Bali, and Nusa Tenggara, there has been a noticeable absence of studies examining meteorological droughts. As a result, this study holds a pioneering status, representing the initial endeavor to project meteorological drought characteristics under CMIP6 scenarios in these regions. In details, this study aims to: 1) identifying changes on rainfall in Java, Bali, and Nusa Tenggara islands based on existing conditions and in the future based on CMIP6 climate scenarios, and 2) assessing the climate change impact on the change on frequency, duration, and intensity of meteorological drought. This study uses rainfall data from six climate models from the Coupled Model Intercomparison Project Phase 6 (CMIP6), consisting of SSP245 and SSP585 scenarios. The CMIP6 model output rainfall was corrected with observational rainfall data through the Linear Scaling (LS) correction method to minimize the overestimated value of the model rainfall. Observed rainfall data was obtained from 20 BMKG rainfall observation stations in the study area. Meteorological drought was analyzed using the Standardized Precipitation Index (SPI) on a 3-month scale (SPI-3) to determine the characteristics of meteorological drought, including frequency, duration, and intensity.

2. STUDY AREA

The study area includes the mainland territories of Java, Bali, and Nusa Tenggara, situated within the geographical coordinates of 105°09'98" E – 125°19'33" E longitude and 5°04'88" S – 11°00'76" S latitude as shown in **Fig.1**. These islands collectively occupy an area of 206.910 km^2, with Java, Bali and Nusa Tenggara Islands covering 134.815 km^2, 5.589 km^2, and 66.506 km^2, respectively. In terms of climate, the monthly rainfall patterns in these Islands exhibit higher precipitation levels from December to March, contrasting with lower rainfall from June to October. This indicates that the wet and dry seasons in the study area primarily occur from December to March, and from June to October. The average monthly and annual rainfall values recorded at each monitoring station are shown in **Table 1**.

Table 1.

Average Monthly and Annual Rainfall in Java, Bali, and Nusa Tenggara from 2000 to 2015 (*Source: Analysis result of BMKG rainfall data, 2023*).

Island	Monthly Average (mm)												Annual Average (mm)
	Jan	Feb	Mar	Apr	May	Jun	Jul	Aug	Sep	Oct	Nov	Dec	
Java	326	303	241	180	135	90	55	26	37	98	208	273	1,972
Bali	403	259	231	151	79	41	30	15	32	59	111	316	1,727
Nusa Tenggara	273	280	239	140	66	25	14	22	51	101	190	261	1,659

Java, Bali, and Nusa Tenggara Islands experience a consecutive annual rainfall of 1,971 mm, 1,727 mm, and 1,659 mm every year. The highest monthly average rainfall was recorded in January, relatively 310 mm/month, while the least was observed in August, with figures of 26 mm/month, 15 mm/month, and 22 mm/month, for Java, Bali, and Nusa Tenggara, respectively.

3. DATA AND METHODS

3.1. Data

Historical rainfall data obtained from the Indonesian Bureau of Meteorology, Climatology, and Geophysics (BMKG) Online Data Portal was accessed through the BMKG website https://dataonline.bmkg.go.id/akses_data. This included the daily rainfall measurements from 2001 to 2015, which were determined based on the data availability at each observation station. To accurately represent the climatic conditions at the study locations, 20 observation stations were carefully selected based on data availability. The distribution of these stations across the study area is shown in **Fig. 2**, where each point was labelled with a number, to facilitate the analysis process. In addition, the details for each station are shown in **Table 2**.

Table 2.

BMKG Station Number, Name, and Location used in the Study.
(Source: BMKG, 2023).

Stat. Numb.	Stat. Code	Stat. Name	Province	Lat.	Lon.	Elev.
1	96739	Budiarto	Banten	-6.28	106.56	42
2	96745	Kemayoran	DKI Jakarta	-6.16	106.84	4
3	96751	Citeko	West Java	-6.69	106.93	920
4	96783	Bandung	West Java	-6.88	107.59	791
5	96791	Kertajati	West Java	-6.73	108.26	85
6	96797	Tegal	Central Java	-6.87	109.12	1
7	96805	Tunggul Wulung	Central Java	-7.72	109.01	8
8	96837	Tanjung Emas	Central Java	-6.95	110.42	2
9	96943	St. Klim. Jawa Timur	East Java	-7.90	112.60	590
10	96935	Juanda	East Java	-7.38	112.78	3
11	96973	Trunojoyo	East Java	-7.04	113.91	3
12	96987	Banyuwangi	East Java	-8.22	114.36	52
13	97230	I Gusti Ngurah Rai	Bali	-8.75	115.17	4
14	97242	Nusa Tenggara Barat	West Nusa Tenggara	-8.64	116.17	55
15	97260	Sultan Muhammad Kaharuddin	West Nusa Tenggara	-8.49	117.41	3
16	97270	Sultan Muhammad Salahuddin	West Nusa Tenggara	-8.54	118.69	5
17	97340	Umbu Mehang Kunda	East Nusa Tenggara	-9.67	120.30	10
18	97284	Frans Sales Lega	East Nusa Tenggara	-8.63	120.45	1070
19	97310	Gewayantana	East Nusa Tenggara	-8.27	122.99	9
20	97372	Eltari	East Nusa Tenggara	-10.17	123.67	102

The present study used CMIP6 climate model data covering the period from 2001 to 2060, downloaded from the website https://esgf-node.llnl.gov/search/cmip6/. In addition, six specific climate models from the CMIP6 dataset were selected, and three different experiments were conducted, namely historical, SSP2, and SSP5. The historical experiment was carried out to correct baseline data using historical information, while the SSP2 and SSP5 scenarios were adopted for future projection analysis. The CMIP6 models for this study were selected based on the availability of precipitation (p) variables at the first variant level (r1i1p1f1) and a resolution of 100 km, with detailed information shown in **Table 3**.

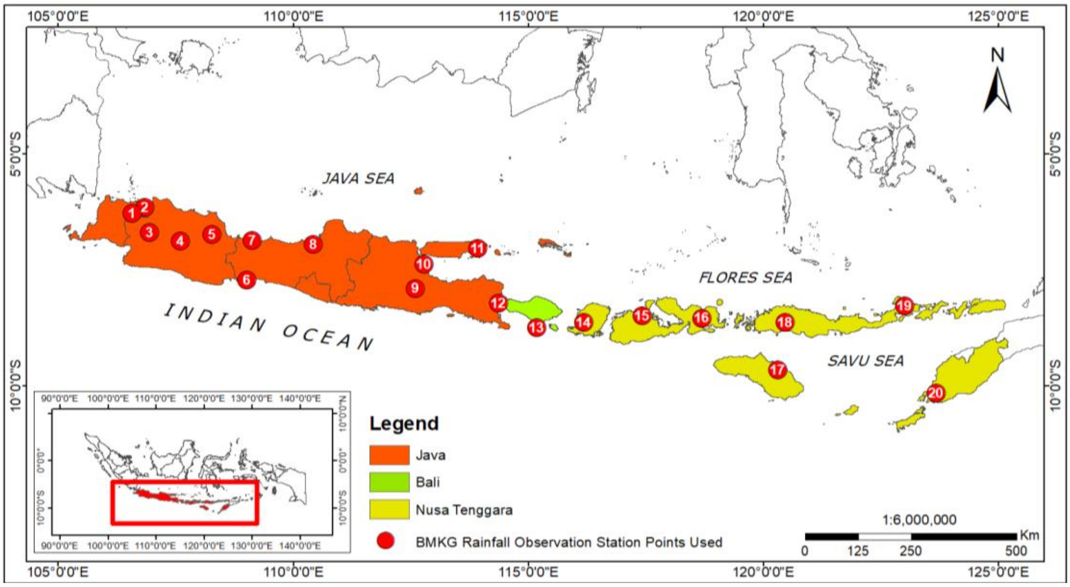

Fig. 2. Map of BMKG Rainfall Observation Station Distribution
(Source: Analysis result of BMKG rainfall data, 2023).

Table 3.

List of CMIP6 Models Used in Study (Source: CMIP6 data portal, 2023).

No.	Model	Variant	Experiment	Period	Variable	Frequency	Resolution
1	CAMS-CSM	r1i1p1f1	*Historical* SSP2 SSP5	2001 – 2015 2016 – 2060	Pr	daily	100 km
2	CESM2-WACCM	r1i1p1f1	*Historical* SSP2 SSP5	2001 – 2015 2016 – 2060	Pr	daily	100 km
3	CanESM5	r1i1p1f1	*Historical* SSP2 SSP5	2001 – 2015 2016 – 2060	Pr	daily	100 km
4	GFDL-CM4	r1i1p1f1	*Historical* SSP2 SSP5	2001 – 2015 2016 – 2060	Pr	daily	100 km
5	MPI-ESM1-2-HR	r1i1p1f1	*Historical* SSP2 SSP5	2001 – 2015 2016 – 2060	Pr	daily	100 km
6	MRI_ESM2	r1i1p1f1	*Historical* SSP2 SSP5	2001 – 2015 2016 – 2060	Pr	daily	100 km

3.2. Processing of the CMIP6 Climate Model Rainfall Data

A regridding process was conducted to obtain rainfall values that can accurately represent the precipitation at the study location in comparison to the BMKG observation station points. This process entailed the use of Bilinear Interpolation method to match the CMIP model data with the nearest BMKG station locations. Bilinear Interpolation is a resampling method that uses the weighted average distance from the four nearest pixel center values to ascertain the new point. Unlike the Nearest Neighbors method, which assigns the value of the new pixel center point based on that of the nearest pixel center point, Bilinear Interpolation takes into account the distances to the four nearest points weighting it accordingly, and then averaging the weighted values. In this context, the pixel center points refers to that of the centroid found in the CMIP6 models.

Bias correction serves as a critical step in improving the model spatial resolution and ensuring it is consistent with the historical data (Faqih, 2017). However, of the available methods, the Linear Scaling (LS) bias correction is the simplest, and primarily focuses on ensuring the mean of the raw model is consistent with the observed values (Kurnia et al., 2020). To obtain the bias-corrected rainfall prediction for the m-month ($Pcor,m$), it is necessary to establish the relationship between the observed mean μ ($Pobs,m$) and that of the model μ ($Praw,m$) for the same month during the observation period. This relationship led to the effective determination of the correction factor.

The correction factor was applied by multiplying the raw rainfall prediction for the m-month ($Praw,m$). In addition, the LS bias correction produced accurate results in line with the observed values (Kurnia et al., 2020). It is obtained using the following equation (Piani et al., 2010).

$$Pcor,m = Praw,m + \frac{\mu\,(Pobs,m)}{\mu\,(Praw,m)}$$

where: $Pcor,m$ = Bias – corrected rainfall; $Praw,m$ = Model rainfall; $\mu(Pobs,m)$ = Observed mean; $\mu(Praw,m)$ = Model mean

Bias correction requires sufficient data to represent the reference climatological conditions. It typically includes using data spanning a minimum of 10 years (often 30 years) to account for variations over a specific time scale (Met Office, 2018). Due to the limitations of available data for each observation station, this study used 15 years of monthly data from 2001 to 2015, as the baseline correction. The differences in rainfall both before and after correction are shown in **Fig. 3**. The distribution of information regarding the monthly rainfall model (in mm), from 2015 to 2060 is shown in **Fig. 3.** This data is presented for both SSP2 and SSP5 scenarios before (left) and after (right) correction.

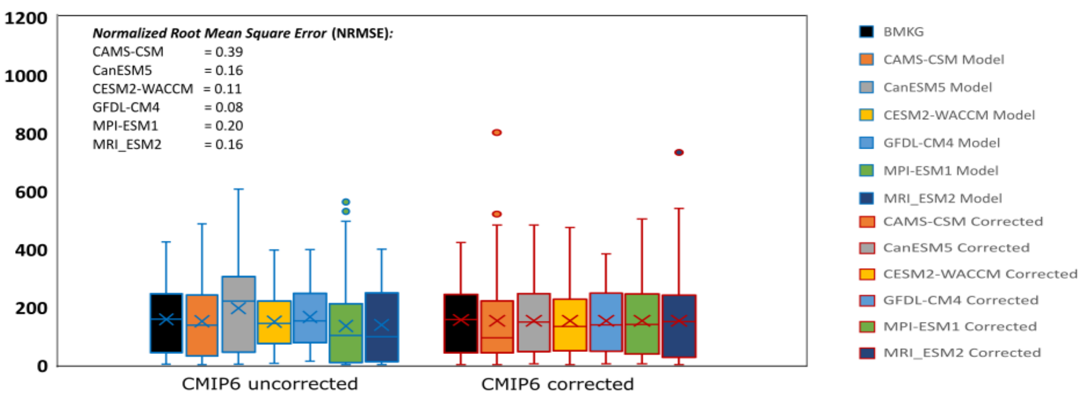

Fig. 3. Box Plot Distribution of Monthly Rainfall Values for CMIP6 Climate Models Before and After Corrected with Historical Data, and The NRMSE values (*Source: Data Processing, 2023*).

In this figure, box plots are used to depict the range of monthly rainfall values for both SSP2 (left) and SSP5 scenarios (right), alongside historical rainfall represented in black. Before the correction, the time series of monthly rainfall in both scenarios exceeded the historical rainfall values (overestimate). However, after correction, the bias-corrected rainfall values for the SSP2 and SSP5 scenarios tend to be in line with the observed patterns throughout the study period, with their central values approaching that of the historical. Based on the correction of error values using the Normalized Root Mean Square Error (NRMSE) method, the best models identified are CanESM5, CESM2, GFDL–CM4, and MRI–ESM5, were identified as the best models. These top four models were subsequently subjected to further analysis in accordance with the study objectives.

3.3. Standardized Precipitation Index

The Standardized Precipitation Index (SPI) was analyzed using monthly rainfall data from historical and projected datasets at each annual study scale. The SPI calculations were performed using a 3-month scale (SPI-3), following the method proposed by McKee et al. (1993), which is in line with the following equation:

$$SPI = \begin{cases} -\left(t - \frac{C_0 + C_1 t + C_2 t^2}{1 + d_1 t + d_2 t^2 + d_3 t^3}\right), t = \sqrt{In\left(\frac{1}{(H(x))^2}\right)}, 0 < H(x) \leq 0{,}5 \\ \left(t - \frac{C_0 + C_1 t + C_2 t^2}{1 + d_1 t + d_2 t^2 + d_3 t^3}\right), t = \sqrt{In\left(\frac{1}{(H(x))^2}\right)}, 0{,}5 < H(x) \leq 1 \end{cases}$$

where *H(x) represents the cumulative gamma distribution, while C and D are constants.*

The value of H(x) is determined by the following equation:

$$H(x) = q + (1 - q)G(x)$$

where *q is the probability of zero rainfall (no rainfall occurrence), calculated based its frequency in the study time scale.*

Meanwhile, G(x) is the cumulative probability of the gamma distribution for non-zero rainfall values. Its value is calculated using the following equation:

$$G(x) = \frac{1}{\beta^{\alpha}\Gamma(\alpha)} \int_0^x x^{a-1} e^{-x/\beta} dx$$

where *α, β, x and Γ(α) are the shape parameter, controls the scale, the variable representing precipitation amount, and the gamma function, respectively.*

In this study, the Standardized Precipitation Index (SPI) for a 3–month time scale (SPI–3) was analyzed. This index allows for the evaluation of meteorological drought conditions related to rainfall anomalies. The SPI was originally developed by McKee et al. (1993), and its classifications are shown in **Table 4**.

Table 4.

SPI Classification (*Source: McKee et al. 1993*).

SPI Value	Classification
> 2.00	Extremely Wet
1.50 – 1.99	Wet
1.00 – 1.49	Moderately Wet
-0.99 – 0.99	Normal
-1.00 – -1.49	Moderately Dry
-1.50 – -1.99	Dry
< -2.00	Extremely Dry

3.4. Drought Characteristics

Drought characteristics were described based on the analysis of SPI calculations (Mckee et al., 1993). The scale of negative and positive values representing different drought conditions is shown in **Fig. 4**. Specifically, drought is presumed to occur when the SPI value falls below -1.00. With the drought classification definition provided by McKee et al. (1993) in **Table 4**, its characteristics can be determined, including frequency, duration, and intensity. An illustrative representation of these drought characteristics is shown in **Fig. 4**.

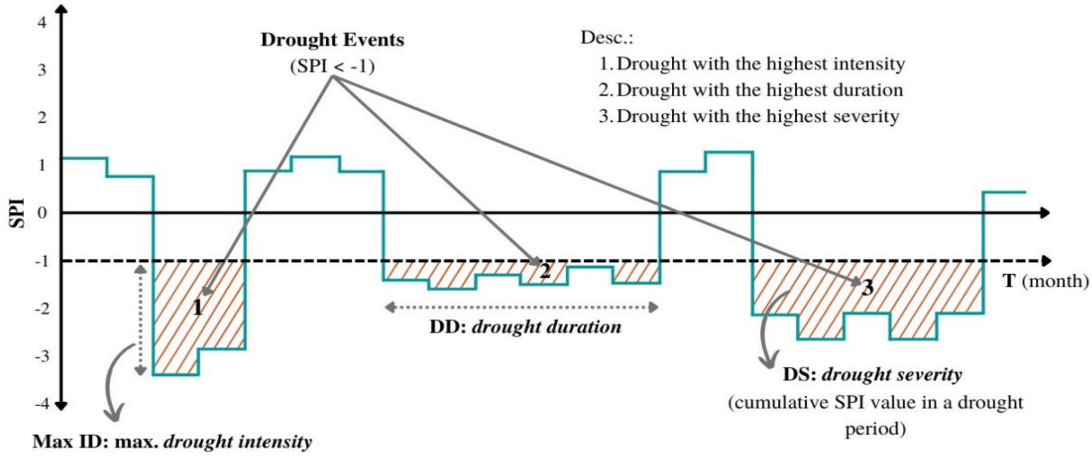

Fig. 4. Drought Characteristics Scheme based on SPI Value (*Source: Data Processing, 2023*).

4. RESULTS

4.1. Changes in Rainfall Based on Climate Change Scenarios

The annual rainfall data in Java, Bali, and Nusa Tenggara Islands are shown in **Fig. 5**. The graph illustrates the performance of each dataset from the rainfall models and scenarios used in this study. The data presented includes the average annual rainfall for all stations analyzed within the study location. The average annual rainfall for the years 2001 to 2015 represents historical data obtained from BMKG observation stations. Meanwhile, for the years 2016 to 2060, it was analyzed using the six CMIP6 models. Each of these CMIP6 models was assessed under two scenarios, namely SSP245 and SSP585. In the graphical representation, the SSP245 and SSP585 scenarios are depicted using solid, and dashed lines, respectively.

In general, both historical rainfall and CMIP6 model data for each scenario exhibit fluctuating patterns within a range of 700 to 3700 mm annually. When compared to the historical data from 2001 to 2015, the CMIP6 model for each scenario showed greater variability. It was observed that the SSP245 and SSP585 scenarios for the same model exhibited similar graph patterns. For example, the CanESM5 model data (light green line) in the SSP245 scenario indicated lower values in the early 2020s, followed by an increase at the beginning of 2040, while in the SSP585 these remained relatively stable. The CESM2-WACCM model data (yellow line) showed fluctuations that ranged from lower to higher compared to historical data. Furthermore, the GFDL-CM4 model data (light blue line) exhibited an upward trend from 2040 to 2060. The MRI-ESM 2 model data (purple line) tends to be consistently lower than that of historical and other CMIP6 models.

To avoid bias and uncertainty arising from analyzing varying average rainfall values across different CMIP6 models individually, the significance of utilizing a multi-model ensemble (MME) approach, was emphasized (Seker & Gumus, 2022). The temporal change trends of the MME in each scenario are shown in **Fig. 6**. The MME for the SSP245 and SSP585 scenarios are shown in a dark blue and red graph with dashed trend lines, respectively.

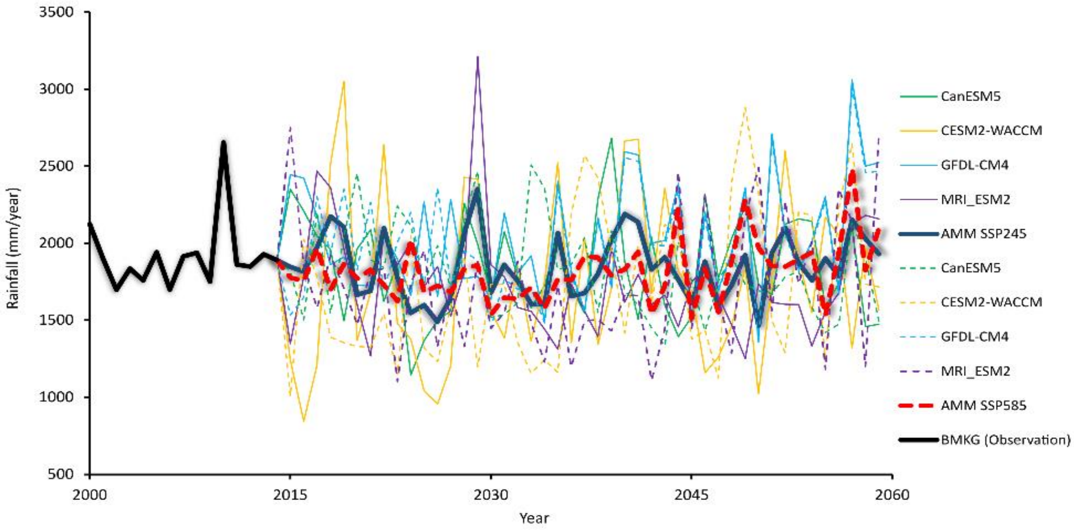

Fig. 5. Graph of Average Annual Rainfall from 2001 to 2060. The 2001 to 2015 Rainfall was based on Historical Data, while the 2016 to 2060 Rainfall was based on the CMIP6 Climate Model (*Source: data processing, 2023*).

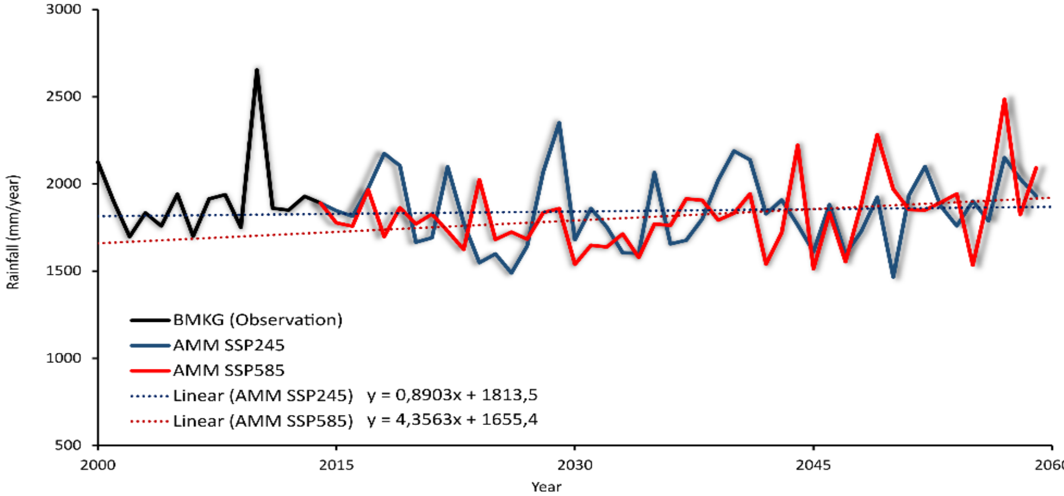

Fig. 6. Graph of Average Annual Rainfall for 2001 to 2060 based on the AAM Climate Model SSP245 and SSP585 Scenarios (*Source: data processing, 2023*).

The examination of annual rainfall trends within the MME for the SSP245 and SSP585 scenarios from 2016 to 2060 shows changes that do not significantly differ from the historical data obtained from 2001 to 2015. According to Faqih et al. (2016), changes in rainfall patterns are anticipated in certain regions of Indonesia in the subsequent years. Some areas, such as the southern parts of Sumatra and Kalimantan, as well as most of Java, Bali, and Nusa Tenggara, are expected to experience a decline in rainfall between 2051 and 2080.

The MME results for the SSP585 scenario indicated a consistent trend of increasing rainfall projections from 2016 onwards, while the projections for SSP245 tend to show a decline from the same period to 2060. This finding is in line with the study conducted by Li et al. (2020), that annual rainfall is expected to slightly increase every decade. Despite the differences in trends between these two scenarios, the gap between them is not significantly large.

Indonesia experienced an average annual temperature of 26.38°C in 2020, an increase of about 0.8°C compared to the temperature recorded in 1901 (Statista, 2023). Rising temperatures have the potential to increased heatwaves and evaporation rates as well as changes in rainfall patterns, significantly impacting Indonesia's ecosystems, water resources and agriculture (Firmansyah et al., 2022). Although the study indicates that there will be a slight increase in rainfall at the research location in the coming decades, it is important to be aware of the changes in rainfall patterns that can disrupt the hydrological cycle. These changes in temperature and rainfall can also have an impact on pests and diseases that affect crops (Ansari et al., 2021). As the leading region for rice production in Indonesia, these altered rainfall patterns in Java, Bali, and Nusa Tenggara may lead to imbalances in rice production and can adversely affect food security at the national level (Gupta et al., 2022).

4.2. Drought Characteristics

The meteorological drought in the study area was analyzed using the SPI-3 (Standardized Precipitation Index) on a 3-month scale. This evaluation was based on four distinct time ranges, the historical or existing years spanning from 2001 to 2015, and that of the projection categorized from 2016 to 2030, 2031 to 2045, and 2046 to 2060. To capture a representative view of the study areas, this analysis was conducted across 20 rainfall observation stations that cover Java, Bali, and Nusa Tenggara. The projection years were evaluated based on the CMIP6 AMM climate model for each scenario. The characteristics of meteorological drought, including frequency, duration, and intensity, were analyzed concerning the modeled SPI-3 results.

Meteorological drought tends to occur when the SPI-3 value is less than the scale of -1 (SPI < -1). Based on the SPI-3 modeling analysis, there was a general increase in the occurrence of meteorological drought in the study area for both the SSP245 and SSP585 scenarios compared to the historical data. The drought patterns under these scenarios show a similar trend, with related events occurring at almost all stations annually, with only slight variations in their severity. Comprehensive details regarding the analysis of meteorological drought are presented in the following sections.

4.3. Drought Frequency

The changes in drought frequency under the SSP245 scenario in the Java region are projected to increase twice or three times in each study time scale, with an average occurrence of 13 times from 2016 to 2030, and 14 times from 2031 to 2045 and 2046 to 2060. The frequency of drought in Bali is expected to decrease compared to the historical time scale, with an average of 14 occurrences from 2016 to 2030, and 15 occurrences from 2031 to 2045 and 2046 to 2060. In the Nusa Tenggara region, the average frequency of drought was projected to increase by one to two occurrences. From 2016 to 2030, the average drought occurrences tend to be 14, and during the periods of 2031 to 2045 and 2046 to 2060, it is expected to occur 15 times. Conversely, under the SSP585 scenario, all three regions Java, Bali, and Nusa Tenggara were estimated to experience 15 drought occurrences each from 2016 to 2030, 2031 to 2045, and 2046 to 2060.

Spatial changes were illustrated through color variations at different stations, each representing the study area within various climate scenarios. The distribution of meteorological drought frequencies in Java, Bali, and Nusa Tenggara from 2000 to 2060 is shown in **Fig. 7**. The frequency analysis was conducted by counting the number of drought events that occurred in each time scale. The analysis revealed a significant pattern, with a consistent increase in drought frequency when transitioning from the historical to the projection period. Furthermore, this increase is particularly pronounced in the SSP585 scenario. During the historical period, the highest frequency of drought was observed in Bali, with a smaller portion affecting western Nusa Tenggara. The lowest frequency of drought events was recorded in the southern and eastern parts of Java.

In the projection period, a similar frequency of drought events was observed for both the SSP245 and SSP585 scenarios, averaging approximately 10 to 15 drought events per station. However, the probability graphs of drought frequency exhibit variations between these two scenarios across different projection time scales. The probability concept in this context refers to the likelihood of drought events occurring within a certain time frame. It serves as a quantitative measure to assess the possibility of droughts occurring during the study period at each station.

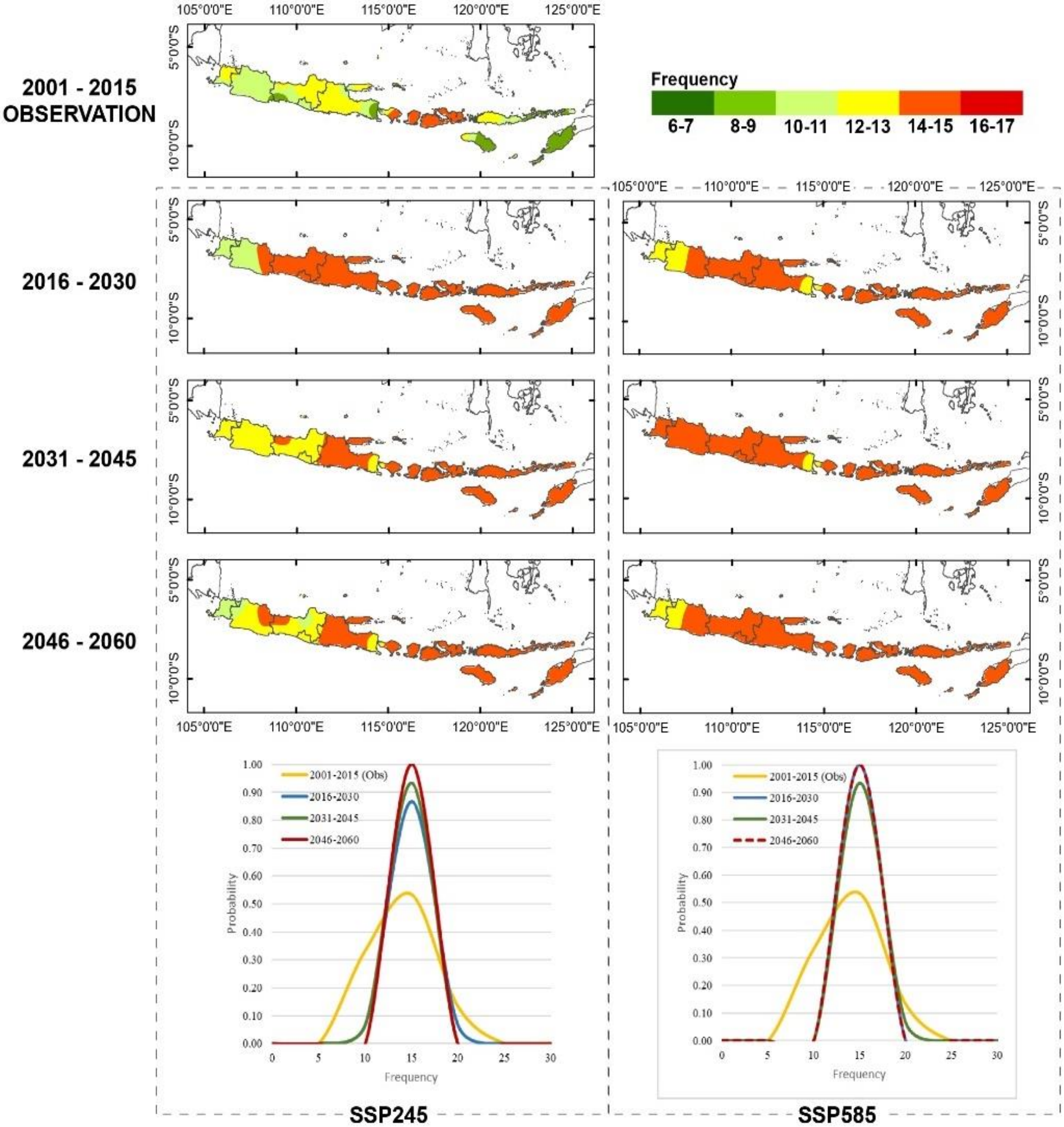

Fig. 7. Meteorological Drought Frequency Distribution for 2001 to 2015 based on Historical Data and 2016 to 2060 based on CMIP6 Climate Model SSP245 and SSP585 Scenarios (Source: data processing, 2023).

The SSP245 scenario showed that the highest frequency of drought events occurred 15 times for each study time scale. From 2016 to 2031, a frequency of 15 drought occurrences with a probability of 0.87, was recorded. This probability increased to 0.93 for the subsequent timeframe of 2031 to 2045. Finally, from 2046 to 2060, the probability reached its maximum, at 1.0. The SSP585 scenario also showed that the highest number of drought events occurred 15 times during each time scale. The highest probabilities were recorded from 2016 to 2030 and 2046 to 2016, with a probability of 1.0. For the 2031 to 2045 timeframe, the probability of observing 15 occurrences is 0.93. Therefore, there is a clear trend of higher drought occurrence under the SSP585 scenario.

4.4. Drought Duration

Drought duration analysis was conducted by calculating the total length, measured in months of drought periods occurring within each time range for every station. According to the SPI-3 analysis, drought events in the study area exhibited an increase in duration under both the SSP245 and SSP585 climate scenarios compared to the historical period. Java, Bali, and Nusa Tenggara experienced the maximum or longest recorded drought duration during the historical period. Specifically, Java endured droughts lasting for 37 months, while Bali and Nusa Tenggara experienced durations of 30 months each. The shortest recorded drought duration during this historical period was eight and 15 months in Java and Nusa Tenggara, respectively.

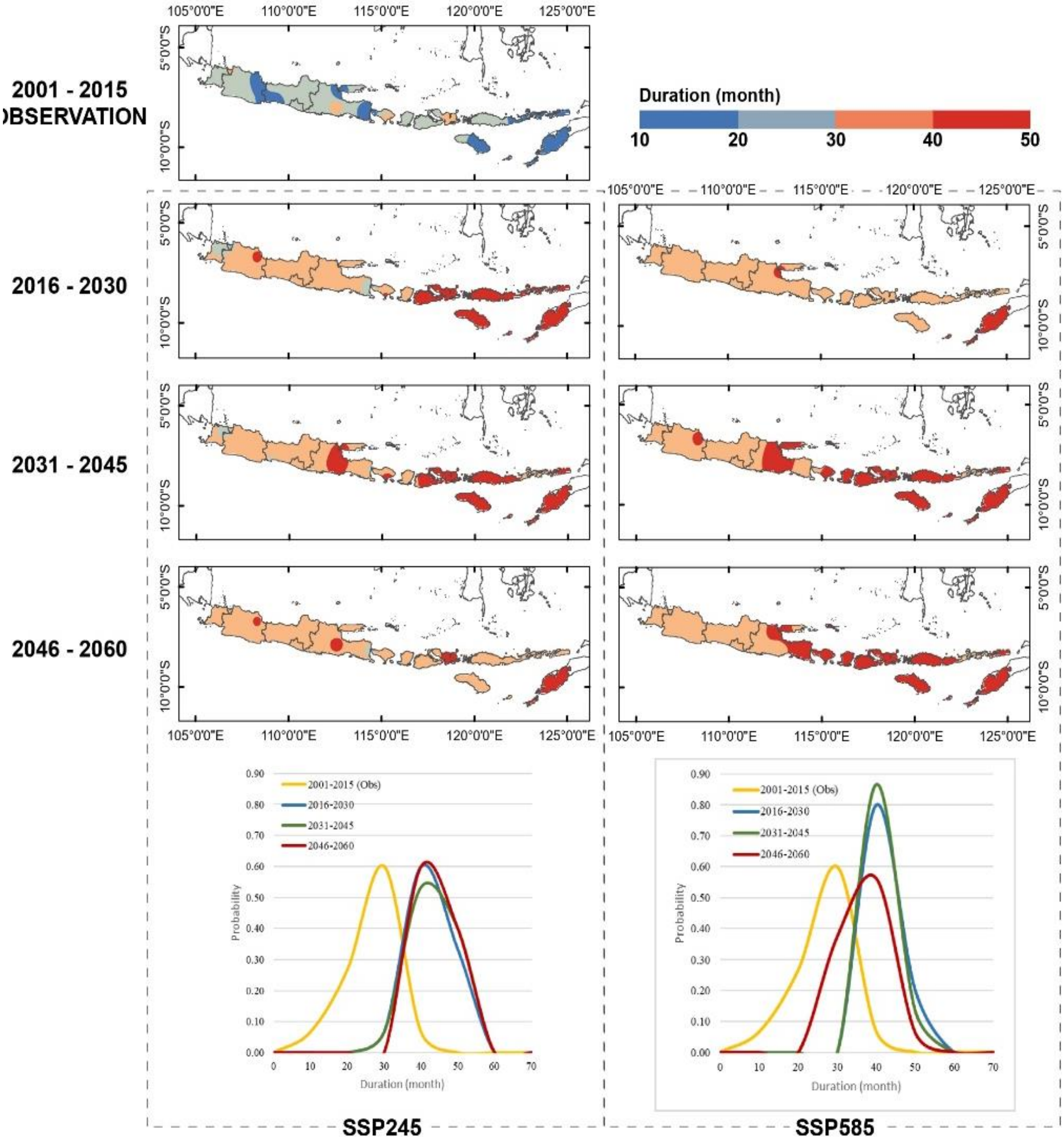

Fig. 8. Meteorological Drought Duration Distribution for 2001 to 2015 based on Historical Data and 2016 to 2060 based on CMIP6 Climate Model SSP245 and SSP585 Scenarios (*Source: data processing, 2023*).

Under the SSP245 scenario, an increase was observed in the maximum drought duration experienced in Java, Bali, and Nusa Tenggara. During the 2016 to 2030 time range, the maximum drought duration extended to 40, 30, and 43 months, respectively. This trend continued in the 2031 to 2045 period, with durations reaching 41, 43, and 45 months. In the 2046 to 2060 time frame, these durations were recorded at 42, 42, and 43 months. Meanwhile, in the SSP585 scenario, they each experienced a similar increase in drought duration for these regions. In the 2016 to 2030 period, the maximum durations were 41, 32, and 42 months. This pattern persisted into the 2031 to 2045 timeframe, with durations of 39, 32, and 47 months. Finally, in the 2046 to 2060 period, maximum drought durations were 41, 32, and 44 months. Nusa Tenggara consistently experienced the longest drought durations in both scenarios.

The distribution of meteorological drought duration in Java, Bali, and Nusa Tenggara is shown in **Fig. 8**. According to the SPI-3 modeling results, the drought duration increases over time. This trend is evident in the distribution pattern of drought duration across different time ranges. In the SSP245 scenario, for each projection time range, a longer drought duration was observed in the eastern part of Java, Bali, alongside the western region of Nusa Tenggara. However, during the 2046 to 2060 timeframe, it appears that the drought duration increased uniformly across these three study regions. In the SSP585 scenario, there was an increase in drought duration during the 2016 to 2030 period in a small part of western Java. This was followed by a shift towards increased drought duration in the southern part of Nusa Tenggara during the 2031 to 2045 period. The increase in drought duration became more uniform across the three study regions during the 2045 to 2060 period.

Probabilities were used to measure the likelihood of drought persisting in a specific region or area during a certain time interval. These were used to estimate how likely it is for droughts to occur during the time scale before returning to normal conditions. The probability graphs in **Fig. 8** showed a significant shift between the historical and projection periods under the SSP245 and SSP585 scenarios. The historical period indicated that droughts were more likely to last for 30 months, with a probability of 0.60. However, the scenario shifted under SSP245, where it was more likely to last for a duration of 40 months and a probability of 0.60 during 2016 to 2030 and 2046 to 2060 periods. In the 2031 to 2045 period, the probability decreased slightly to 0.53 for the same 40-month droughts. Under the SSP585 scenario, the occurrence of droughts during 2016 to 2030 and 2031 to 2045 periods were more likely to last for 40 months and a high probability of 0.87. During the 2046 to 2060 period, a more frequent occurrence of 40-month droughts was observed, with a probability of 0.56. It was projected that drought durations tend to frequently last for 40 months, with a higher likelihood of occurrence in the SSP585 scenario during 2016 to 2030 and 2031 to 2045 periods.

4.5. Drought Intensity

Drought intensity is assessed by averaging all related events at each observation station within the diverse time range studied. The SPI-3 meteorological drought modeling results indicated that its intensity fell within the moderately dry to dry classifications. However, the temporal changes across different time ranges indicated a decrease in drought intensity observed at most stations. This trend holds for both the SSP245 and SSP585 scenarios when compared to the historical period.

In the historical time range, Java, Bali, and Nusa Tenggara experienced drought with similar intensities of -1.52, -1.48, and -1.48 respectively. However, under the SSP245 scenario, there were variations, in the 2016 to 2030 period, the recorded drought intensities were -1.52, -1.31, and -1.40 for Java, Bali, and Nusa Tenggara. In the 2031 to 2045 timeframe, the recorded intensities were -1.48, -1.29, and -1.37 for Java, Bali, and Nusa Tenggara, respectively. For the 2046 to 2060 period, the drought intensities remained relatively stable at -1.48, -1.29, and -1.39 for Java, Bali, and Nusa Tenggara under the SSP245 scenario. Under the SSP585 scenario, the intensity patterns were slightly similar. During the 2016 to 2030 period, the recorded intensities were -1.48, -1.31, and -1.42 for Java, Bali, and Nusa Tenggara. In the subsequent 2031 to 2045 period, these values changed to -1.49, -1.33, and -1.37, respectively. Finally, in the 2046 to 2060 timeframe, the recorded intensities were -1.50, -1.34, and -1.39 for Java, Bali, and Nusa Tenggara, respectively, under the SSP585 scenario.

The distribution of drought intensity in the study area is shown in **Fig. 9**. Spatially, the intensity of drought during the historical period, classified as dry, was concentrated in the central to western parts of Java. Meanwhile, the eastern side of the study area exhibited a more evenly distributed moderately dry-to-dry intensity. In the SSP245 scenario, there was a significant transition in intensity from dry to moderately dry, spanning from 2016 to 2030 till the 2046 to 2060 period. Conversely, the SSP585 scenario tends to shift from dry to moderately dry intensity relative to the historical period, but there seems to be no significant change across the different projection time scales.

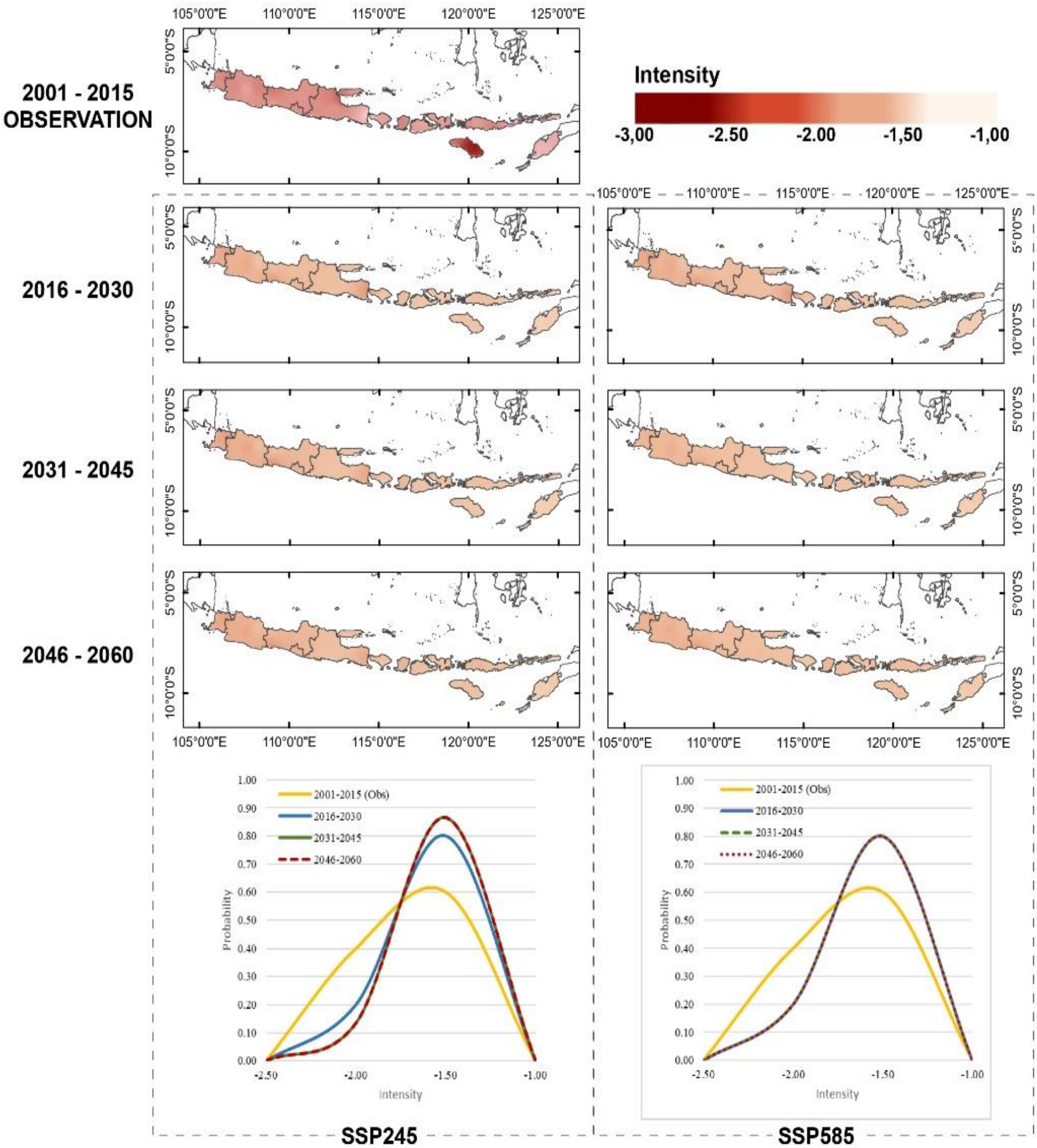

Fig. 9. Meteorological Drought Intensity Distribution for 2001-2015 based on Historical Data and 2016-2060 based on CMIP6 Climate Model SSP245 and SSP585 Scenarios (*Source: data processing, 2023*).

In this context, drought intensity probabilities refer to the likelihood of experiencing severe drought conditions in a particular region or area. These play a crucial role in understanding the chances of drought severity reaching significant or extreme levels during the study time frame under each scenario. The probability graph showed that during the historical period, drought intensity levels ranged from -1.00 to -2.50, with -1.50 being the most frequent and having a probability of 0.60. Analyzing the following periods under both scenarios, the graph tends to shift to the right, with higher probability peaks compared to the historical period. This indicated that the drought intensity was expected to decrease in the subsequent years. Under the SSP245 scenario, drought intensity during the 2016 to 2030, 2031 to 2045, and 2046 to 2060 periods were more likely to occur at -1.50, with probabilities of 0.80, 0.87, and 0.87, respectively. Similarly, under the SSP585 scenario, drought intensity during these periods was more likely to occur at -1.50, with a probability of 0.80.

5. DISCUSSIONS

Droughts in Java, Bali and Nusa Tenggara region have been occurring and intensifying for decades. The above region is often suffered the most, for example in the 2019 drought event where hundred thousand hectares of agricultural land in Indonesia suffered crop failure (Indonesian Bureau of Statistics, 2020). In detail, crop failure due to drought resulted in the failure of 17,000 hectares of rice fields in West Java and Central Java. While in the previous year, drought hit around 250,000 hectares of agricultural land in the entire country (Amir and Alta, 2022).

The results of the meteorological drought prediction can be used as a basis in assessing the potential and challenges that will occur in the future. The expected increase in drought during the study period indicates the challenges and threats to food security and clean water availability, especially in locations with the potential to experience long and intense droughts (Safura, 2023). Water usage management and an innovative agricultural system are two of the most crucial ways to address water scarcity challenges caused by drought (Firmansyah et al., 2022). Policymakers need to consider appropriate adaptation and mitigation efforts to increase agricultural productivity in the middle of drought conditions that hit the study area. For example, making effective land and crop management practices, regulating irrigation strategies by considering the availability of water resources, mapping crop growth potential in specific locations with predictions of the amount of crop production that will be produced, and optimizing resource allocation in order to increase agricultural productivity (Sekaranom et al., 2022).

The prediction of future drought potential can also serve as an early warning to assist farmers in taking quick and appropriate actions to minimize potential crop losses. For instance, by managing irrigation, selecting suitable crop types, scheduling planting, and providing fertilizers (Nurjani et al., 2020). Social adaptation strategies to cope with drought due to climate change have been implemented by farmers in several regions of Indonesia. For example, in Kebumen area (Central Java), farmers have adopted various adaptation strategies to address the impact of climate change on the agricultural sector (Sekaranom et al., 2021). At present, more than 85% of the farmers switch to more climate-tolerant crop varieties. Furthermore, almost all (94%) farmers are attempting to maintain productivity through adjustments to the local planting calendar.

6. CONCLUSIONS

This study examined changes in rainfall and meteorological drought characteristics by analyzing historical data and future projections using SPI-3 analysis under the CMIP6 climate scenarios. The analysis covered Java Island, Bali, and Nusa Tenggara and comprised four time periods, namely historical data spanning from 2001 to 2015 and projections for the years 2016 to 2030, 2031 to 2045, and 2046 to 2060. The results of the analysis were summarized as follows:

1. The evaluation of projected rainfall data, obtained from the four CMIP6 climate models for each scenario, revealed significant variability over time. During the study period, the average rainfall in the SSP245 scenario was projected to have an increasing trend compared to historical years. In the SSP585 scenario, the projected trend indicated a higher increase in rainfall relative to historical

years. Spatially, both scenarios exhibited a decrease in rainfall compared to historical periods, but there were no significant changes across the various timeframes within each scenario.

2. The increase in meteorological drought occurrences was evident in the study area under both the SSP245 and SSP585 scenarios compared to the historical period. Drought frequency exhibited an upward trend, with a growing number of events projected during the study period. This trend was particularly pronounced under the SSP585 scenario. Future droughts were predicted to have longer durations in both scenarios, specifically in the Nusa Tenggara region. Drought intensity was also predicted to decrease in both scenarios relative to historical periods. Therefore, the number of drought occurrences in the future is expected to increase in the study area, with longer durations, while the absolute value of its intensity diminishes. The increase in drought occurrences was more pronounced under the SSP585 scenario.

In the context of characterizing drought under climate change scenarios through regional analysis, it relies on specific climate scenarios, namely SSP245 and SSP585 which may not encompass the full range of potential climate outcomes. These scenarios are just two possibilities among other climate pathways that could significantly impact our results. Additionally, our study primarily focuses on regional-scale analysis, and it may not capture local-scale variations in drought characteristics. Furthermore, the research is based on assumptions and data available at the time, and as climate science evolves, our understanding of drought patterns and their interaction with climate change may change. Despite these limitations, the study provides valuable insights into the impact of climate change on drought in the study area and serves as a foundation for further research in the region.

ACKNOWLEDGMENT

This study was supported by "Hibah Rekognisi Tugas Akhir 2023" Universitas Gadjah Mada, Indonesia with contract number: 5075/UN1.P.II/Dit.-Lit/PT/01/01/2003, dated 12th May 2023, and principal investigator Dr. Sc. Andung Bayu Sekaranom., M.Sc.

REFERENCES

Adhyani, N. L., June, T., & Sopaheluwakan, A. (2017) Exposure to Drought: Duration, Severity and Intensity (Java, Bali and Nusa Tenggara). *IOP Conference Series: Earth and Environmental Science*, 58, 012040.

Amir, M. F., & Alta, A. (2022) *Water Scarcity Threatens our Food: From Competition to Unequal Access. Center for Indonesian Policy Studies.* Last access on October 26, 2023. https://www.cips-indonesia.org/post/water-scarcity-threatens-our-food-from-competition-to-unequal-access.

Ansari, A., Pranesti, A., Telaumbanua, M., Alam, T., Wulandari, R. A., & Nugroho, B. D. A. (2023) Evaluating the effect of climate change on rice production in Indonesia using multimodelling approach. *Heliyon*, 9, e19639

BMKG (2023). *Data Online BMKG*. Last access on May 1, 2023. https://dataonline.bmkg.go.id/

Bock, L., Lauer, A., Schlund, M., Barreiro, M., & Bellouin, N. (2020) Quantifying Progress Across Different CMIP Phases with the ESMValTool. *Journal of Geophysical Research: Atmospheres,* 6, e2019JD032321.

CMIP6 data portal (2023) *World Climate Research Programme CMIP6*. Last access on May 1, 2023. https://esgf-node.llnl.gov/search/cmip6/.

Cook, B. I., Mankin, J. S., Marvel, K., Williams, A. P., Smerdon, J. E., & Anchukaitis, K. J. (2020) Twenty-First Century Drought Projections in the CMIP6 Forcing Scenarios. *Earth's Future,* 8, e2019EF001461.

EM-DAT (Emergency Event Database) (2021) *Extreme events defining our lives Executive summary*. Centre for Research on the Epidemiology of Disasters. https://doi.org/10.1787/eee82e6e-en

Eyring, V., Bony, S., Meehl, G. A., Senior, C. A., Stevens, B., Stouffer, R. J., & Taylor, K. E. (2016) Overview of the Coupled Model Intercomparison Project Phase 6 (CMIP6) experimental design and organization. *Geoscientific Model Development,* 9, 1937–1958.

Faqih, A. (2017) A Statistical Bias Correction Tool for Generating Climate Change Scenarios in Indonesia based on CMIP5 Datasets. *IOP Conference Series: Earth and Environmental Science,* 58, 012051.

Faqih, A., Hidayat, R., Jatmiko, S., & Radini. (2016) Climate modeling and analysis for Indonesia 3rd national communication (TNC): Historical and climate and future climate. *Final Report*. Ministry of Environment and Forestry (MoEF). United National Development Programme (UNDP) And BoG.

Firmansyah, A. J., Nurjani, E., & Sekaranom, A. B. (2022) Effects of the El Niño-Southern Oscillation (ENSO) on rainfall anomalies in Central Java, Indonesia. *Arabian Journal of Geosciences,* 15(24), 1746.

GSHHG (2017) *A Global Self-consistent, Hierarchical, High-resolution Geography Database (GSHHG)*. Last access on May 1, 2023. https://www.soest.hawaii.edu/pwessel/gshhg/.

Gupta, D., Gujre, N., Singha, S., & Mitra, S. (2022) Role of existing and emerging technologies in advancing climate-smart agriculture through modeling: A review. *Ecological Informatics,* 71, 101805.

Ha, T. V., Huth, J., Bachofer, F., & Kuenzer, C. (2022) A Review of Earth Observation-Based Drought Studies in Southeast Asia. *Remote Sensing,* 14, 3763.

Held, I. M., & Soden, B. J. (2006) Robust Responses of the Hydrological Cycle to Global Warming. *Journal of Climate,* 19, 5686–5699.

Huang, J., Wang, Y., Fischer, T., Su, B., Li, X., & Jiang, T. (2016) Simulation and projection of climatic changes in the Indus River Basin, using the regional climate model COSMO-CLM. *International Jurnal Climatology,* 37, 2545–2562.

Indonesian Bureau of Statistics (2023) *Harvest Area and Rice Production in Indonesia 2022* (in bahasa). Jakarta: Indonesian Bureau of Statistics.

Indonesian Bureau of Statistics (2020) *Harvest Area and Rice Production in Indonesia 2019* (in bahasa). Jakarta: Indonesian Bureau of Statistics.

IPCC (Intergovernmental Panel on Climate Change) (2021) *Climate Change 2021: The Physical Science Basis Climate Change 2021*. Intergovernmental Panel on Climate Change. https://doi.org/10.1017/9781009157896

Kang, H., Sridhar, V., Mainuddin, M., & Trung, L. D. (2021) Future rice farming threatened by drought in the Lower Mekong Basin. *Scientific Reports,* 11, 9383.

Kurnia, W. G., Muharsyah, R., & Widiyanto, S. (2020). Performance of European Center Medium Weather Forecast (ECMWF) Model Rainfall Bias Correction in Sulawesi (in bahasa). *Buletin GAW Bariri (BGB),* 1(2), 77-86.

Kuswanto, H., & Rahadiyuza, D. (2018) Multi Model Calibration of Rainfall Forecasts in East Nusa Tenggara Using Ensemble Model Output Statistics. *Journal of Physics: Conference Series,* 1028, 012231.

Li, H., Li, Z., Chen, Y., Xiang, Y., Liu, Y., Kayumba, P. M., & Li, X. (2021) Drylands face potential threat of robust drought in the CMIP6 SSPs scenarios. *Environmental Research Letters,* 16, 114004.

Li, S.-Y., Li-Juan, M., Zhi-Hong, J., Guo-Jie, W., Raj, G. K., Jing, Z., Hui, Z., Ke, F., Yu, H.E., & Chun, L. (2020) Projected drought conditions in Northwest China with CMIP6 models under combined SSPs and RCPs for 2015–2099. *Advances in Climate Change Research*, 11(3), 210–217.

Liu, S., Huang, S., Xie, Y., Huang, Q., Leng, G., & Hou, B. (2018) Spatial-temporal changes of maximum and minimum temperatures in the Wei River Basin, China: Changing patterns, causes and implications. *Atmospheric Research*, 204, 1–11.

Mckee, T. B., Doesken, N. J., & Kleist, J. (1993) The relationship of drought frequency and duration to time scales. *Eight Conference on Applied Climatology*, 17(22), 179–183.

Met Office (2018) *UKCP18 Guidance: Bias correction*. Met Office Hadley Centre: Exeter, UK.

Muharsyah, R., & Ratri, D. N. (2015) Drought Duration and Strength Using Standardized Rainfall Index in Bali Island (in Bahasa). *Jurnal Meteorologi Dan Geofisika*, 16(2), 93-104.

Nurjani, E., Harini, R., Sekaranom, A.B. and Mutaqqin, A.S., 2020, March. Tobacco farmers Perspective towards increasing climate change risk on agriculture sector: a case study of Temanggung-Indonesia. *IOP Conference Series: Earth and Environmental Science,* 451(1), 012101.

Parkhurst, H., Nurdiati, S., & Sopaheluwakan, A. (2019) Analysis of drought characteristics in southern Indonesia based on return period measurement. *IOP Conference Series: Earth and Environmental Science*, 299(1), 012050.

Piani, C., Haerter, J. O., & Coppola, E. (2010) Statistical bias correction for daily precipitation in regional climate models over Europe. *Theoretical and applied climatology,* 99, 187-192.

Safura, A. H. (2023) Meteorological Drought Characteristics in Java, Bali, and Nusa Tenggara Islands based on CMIP6 Climate Change Scenario (in bahasa). *Bachelor's Thesis*. Indonesia: Universitas Gadjah Mada.

Sekaranom, A. B., Nurjani, E., & Nucifera, F. (2021) Agricultural climate change adaptation in Kebumen, central Java, Indonesia. *Sustainability*, 13(13), 7069.

Sekaranom, A.B., Purnama, I.S., Cahyadi, A., Andika, N., Febriarta, E., Nurjani, E., Firmansyah, A.J., Maghfiroh, A., Larasati, C. and Septyo, N.D. (2022) Analysis of Surface Water Availability to Meet Agricultural Water Demands in Kediri Regency, Indonesia. *ASEAN J. Sci. Technol. Dev,* 39, 111-118.

Seker, M., & Gumus, V. (2022) Projection of temperature and precipitation in the Mediterranean region through multi-model ensemble from CMIP6. *Atmospheric Research,* 280, 106440.

Statista (2023) *Annual mean temperature in Indonesia from 1901 to 2020 (in degrees Celcius).* Last access on October 26, 2023. https://www.statista.com/statistics/1314386/indonesia-annual-mean-temperature.

Ukkola, A. M., De–Kauwe, M. G., Roderick, M. L., Abramowitz, G., & Pitman, A. J. (2020) Robust Future Changes in Meteorological Drought in CMIP6 Projections Despite Uncertainty in Precipitation. *Geophysical Research Letters*, 46, e2020GL087820.

WMO (2021) *2020 was One of Three Warmest Years on Record*. Last access on March 12, 2023. https://public.wmo.int/en/media/press-release/2020-was-one-of-three-warmest-years-record

Xin, X., Wu, T., Zhang, J., Yao, J., & Fang, Y. (2020) Comparison of CMIP6 and CMIP5 Simulations of precipitation in China and the East Asian summer monsoon. *International Jurnal Climatology,* 40, 6423–6440.

Zhai, J., Kumar, S., Fischer, T., Wang, Y., Su, B., & Asia, S. (2020) Future drought characteristics through a multi-model ensemble from CMIP6 over South Asia. *Atmospheric Research,* 246, 105111.

Zhu, H., Jiang, Z., Li, J., Li, W., Sun, C., & Li, L. (2020). Does CMIP6 Inspire More Confidence in Simulating Climate Extremes over China? *Advances in Atmospheric Sciences,* 37(10), 1119–1132.